Polymer Bulletin 59, 31–44 (2007)
DOI 10.1007/s00289-007-0736-2

Polymer Bulletin

Synthesis and Optoelectronic Properties of Random Copolymers Derived from Fluorene and 2,5-Bis(2,1,3-benzothiadiazolyl)silole

Yongqiang Liu, Zhao Chen, Junwu Chen (✉), Feng Wang, Yong Cao

Institute of Polymer Optoelectronic Materials & Devices, Key Laboratory of Specially Functional Materials and Advanced Manufacturing Technology of MoE, South China University of Technology, Guangzhou 510640, China
E-mail: psjwchen@scut.edu.cn

Received: 16 November 2006 / Revised version: 11 January 2007 / Accepted: 15 January 2007
Published online: 30 January 2007 –

Summary

A novel series of soluble conjugated random copolymers (PFO-BTS) derived from 9,9-dioctylfluorene (FO) and bis(2,1,3-benzothiadiazolyl)silole (BTS) were synthesized by Suzuki coupling reactions. The feed ratios of FO to BTS were 99:1, 95:5, 90:10, and 85:15. Chemical structures and optoelectronic properties of the copolymers were characterized by elemental analysis, NMR, UV absorption, cyclic voltammetry, photoluminescence (PL), and electroluminescence (EL). The elemental analyses of the copolymers indicated that FO and BTS contents in the copolymers were very close to that of the feed compositions. Compared with the solution PL, complete PL excitation energy transfer from the PFO segments to the BTS units could be achieved by film PL at lower BTS content. The films of the copolymers exhibited PL quantum yields between 22 and 34%. EL devices with a configuration of ITO/PEDOT/PFO-BTS/Ba/Al demonstrated that the BTS units could serve as powerful exciton traps, giving orange-red EL emissions. The PFO-BTS15 was utilized to fabricate blend-type PLEDs with the PFO, the EL efficiency was improved to 1.37% with a weight ratio of PFO-BTS15 : PFO = 1 : 4.

Introduction

During the recent years, polyfluorene (PF) and its copolymers have become the promising emitters to be utilized in the fabrications of commercial PLEDs because of their highly efficient photoluminescence (PL) and electroluminescence (EL), excellent thermal and oxidative stability, and good solubility in common organic solvents [1-3]. Normally PFs were blue light emitters due to large band gap [4]. Recent results have shown that emission colors of PFs could be tuned in the entire visible-light region by incorporating narrow band gap comonomers into PF backbone [5-18]. Some aromatic cycles, such as 4,7-dithienyl-2,1,3-benzothiadiazole, 2,1,3-benzoselenadiazole, 2,1,3-naphthoselenadiazole, 5,5'-dithienyl-2,2'-bithiazole, bis(thienyl-2-cyanovinyl)benzene, etc. have been utilized to construct red light-emitting PFs by other researchers [14-18].

2,3,4,5-Tetraarylsiloles possess unusual aggregation-induced emissions (AIE) and blue-shifted emission of crystal relative to that of amorphous solid, two PL properties contrary to most organic emitters [19-21]. Excellent EL performances with external quantum efficiencies (η_{EL}) up to 8% have been realized in organic light-emitting diodes (OLEDs) with 2,3,4,5-tetraphenylsiloles as the emissive layer [22]. Unlike the vacuum deposition process in the fabrication of OLEDs, semiconducting polymeric films for PLEDs can be fabricated via simple and fast solution processing such as spin-coating and even printings. Therefore it is desirable to incorporate 2,3,4,5-tetraarylsiloles as the building blocks to construct π-conjugated silole-containing polymers. π-Conjugated copolymers derived from fluorene and 2,3,4,5-tetraarylsilole would combine the merits of the both building blocks. 2,3,4,5-Tetraphenylsilole (PSP) and 2,5-dithienyl-3,4-diphenylsilole (TST), the two 2,3,4,5-tetraarylsiloles with electron-rich 2,5-substituents, have been introduced to construct silole-containing PFs, in which the excitation energy transfer from the fluorene segments to the silole units could be realized [23,24]. The different 2,5-substitutions of the siloles play an important role on the light-emitting properties of the resulting PF copolymers. The PLEDs with copolymers PFO-PSP and PFO-TST as the emissive layer can emit green and red lights, respectively, demonstrating large and facile tuning of EL colors by the 2,5-substituents [23,24].

Though the silole ring is an electron deficient unit, silole-containing polymers with PSP and TST as the building blocks are only p-type, based on their higher mobility of holes than that of electrons in field effect transistors [24,25]. It has been found that siloles with electron deficient pyridine or bipyridine as 2,5-substituents could show excellent electron-transport properties [26]. Therefore, the 2,5-substituents of a silole play an important role on its carrier transport property. 2,1,3-Benzothiadiazole (BT) is an electron deficient heterocycle, and high electron mobility measured by time-of-flight technique has been found for a fluorene-BT alternating copolymer [27]. Attachments of the BT at the 2,5-positions of a silole would improve the electron transport property of a silole. In this work, 1,1-diethyl-3,4-diphenyl-2,5-bis(7-bromo-2,1,3-benzothiadiazol-4-yl-)silole (BTS), a new silole monomer with bulky 2,5-BT substituents, was prepared by a one-pot synthesis route, from which soluble conjugated random PF copolymers PFO-BTS were successfully synthesized by Suziki coupling reactions. The optoelectronic properties such as UV absorption, electrochemical properties, PL, EL of the copolymers were evaluated.

Experimental

Materials

All manipulations involving air-sensitive reagents were performed under an atmosphere of dry argon. All reagents, unless otherwise specified were obtained from Aldrich, Acros, and TCI Chemical Co. and were used as received. All solvents were carefully dried and purified under nitrogen flow.

Instrumentation

^{1}H and ^{13}C NMR spectra were recorded on a Bruker AV 300 spectrometer with tetramethylsilane (TMS) as the internal reference. Molecular weights of the polymers were obtained on a Waters GPC 2410 using a calibration curve of polystyrene

standards, with tetrahydrofuran as the eluent. Elemental analyses were performed on a Vario EL elemental analysis instrument (Elementar Co.). UV-vis absorption spectra were recorded on a HP 8453 spectrophotometer. The PL spectra of the copolymer solutions were obtained on a Jobin Yvon Fluorolog-3 spectrofluorometer. The PL quantum yields of the copolymer films were determined in an Integrating Sphere IS080 (LabSphere) with 405 nm excitation of a HeCd laser (Melles Griot). Film PL spectra and EL spectra were recorded on an Instaspec IV CCD spectrophotometer (Oriel Co.). Cyclic voltammetry was carried out on a CHI660A electrochemical workstation with platinum electrodes at a scan rate of 50 mV/s against a saturated calomel reference electrode with a nitrogen-saturated solution of 0.1 M tetrabutyl-ammonium hexafluorophosphate (Bu_4NPF_6) in acetonitrile (CH_3CN).

Synthesis of Compounds

Compounds 4,7-dibromo-2,1,3-benzothiadiazole (**5**) [28], 2,7-dibromo-9,9-dioctyl-fluorene (**2**) [15], and 2,7-bis(4,4,5,5-tetramethyl-1,3,2-dioxaborolan-2-yl)-9,9-dioctylfluorene (**3**) [15] were prepared according to literatures, and all of them were recrystallized to reach the desirable purity for the next reactions.

*Synthesis of Bis(phenylethynyl)-diethylsilane (**4**)*

Into a two neck flask containing phenylacetylene (4.39 mL, 40 mmol) in 20 mL THF at 0°C was dropwise added 16 mL 2.5M BuLi (40 mmol) in hexane. The mixture was stirred over 30 min at the temperature. Then 3 mL diethyldichlorosilane (20mmol) was dropwise added to the mixture by syringe. The mixture was allowed to further react for 30 min. All volatiles were removed under reduced pressure. The crude product was purified by a column chromatography using petroleum ether as eluent to provide **4** in 70% yield as colorless oil. ^{1}H NMR, (300 MHz, $CDCl_3$), δ (ppm): 7.50 (m, 4H), 7.27 (m, 6H), 1.18 (m, 6H), 0.87 (m, 4H). ^{13}C NMR, (75 MHz, $CDCl_3$), δ (ppm): 132.0, 128.7, 128.1, 122.6, 106.6, 88.7, 7.3, 6.5.

*Synthesis of 1,1-diethyl-3,4-diphenyl-2,5-bis(7-bromo-2,1,3-benzothiadiazol-4-yl-)silole (**6**)*

A mixture of lithium granular (83 mg, 12 mmol) and naphthalene (1.54 g, 12.1 mmol) in THF (12 mL) was stirred at room temperature under argon for 5 h, readily forming lithium naphthalenide (LiNaph). Then bis(phenylethynyl)-diethylsilane **3** (864 mg, 3.0 mmol) in THF (5mL) was added to the solution of LiNaph dropwise over 2 min at room temperature. After stirring for 10 min, the mixture was cooled to 0°C. $ZnCl_2$(tmen) (tmen = *N*,*N*,*N*′,*N*′-tetramethylethylenediamine) (3.0 g, 12 mmol) was added as a solid to the mixture, followed by the dilution with THF (20 mL), giving a black suspension. After stirring for an additional hour at room temperature, the black suspension was dropwise added to the solution of 4,7-dibromo-2,1,3-benzothiadiazole **5** (2.65 g, 9 mmol) and $PdCl_2(PPh_3)_2$ (70 mg, 0.1 mmol). The mixture was heated to 55°C and stirred for 16 h. After a cooling to the room temperature, an aqueous solution of HCl (1 N) was added and the mixture was extracted with ether. The combined extract was washed with brine, dried over $MgSO_4$, and concentrated. The crude product was purified on a silica gel column using a petroleum ether/ dichloromethane mixture (3:1 by volume) as eluent. Compound **6** in light yellow crystals was obtained in a yield of 30% after recrystallization from a toluene/heptane

mixture. ^{1}H NMR, (300 MHz, $CDCl_3$), δ (ppm): 7.56 (d, 2H), 6.95 (m, 6H), 6.80 (m, 6H), 0.98 (m, 10 H). ^{13}C NMR, (75 MHz, $CDCl_3$), δ (ppm): 157.9, 154.6, 153.3, 138.5; 138.3, 134.6, 132.3, 129.6, 128.6, 127.5, 126.7, 110.9, 7.2, 4.5. Anal. Calcd for $C_{32}H_{24}Br_2N_4S_2Si$: C, 53.64; H, 3.38; S, 8.95. Found: C, 53.31; H, 3.54; S, 9.03.

Polymerization

All of the polymerizations were carried out by palladium(0)-catalyzed Suzuki coupling reactions with equivalently molar ratio of the diboronic ester monomer to the dibromo monomers under argon protection. The purifications of the polymers were conducted in air with yields of 77~85%. A typical procedure for the polymerization of copolymer PFO-BTS1 is given below.

Carefully purified 2,7-bis(4,4,5,5-tetramethyl-1,3,2-dioxaborolan-2-yl)-9,9-dioctyl-fluorene **3** (321 mg, 0.5 mmol), 2,7-dibromo-9,9-dioctylfluorene **2** (269 mg, 0.49 mmol) 1,1-diethyl-3,4-diphenyl-2,5-bis(7-bromo-2,1,3-benzothiadiazol-4-yl-) silole **6** (7.2 mg, 0.01 mmol), $(PPh_3)_4Pd(0)$ (6 mg), and several drops of Aliquat 336 were dissolved in a mixture of toluene (10 ml) and aqueous 2 M Na_2CO_3 (2 ml). The solution was refluxed with vigorous stirring for 24 h. At the end of polymerization, small amount of **3** was added to remove bromine end groups, and bromobenzene was added as a monofunctional end-capping reagent to remove boronic ester end group. The mixture was then poured into vigorously stirred methanol. The precipitated solid was filtered and washed for 24 h with acetone to remove oligomers and catalyst residues. Yellow powder of PFO-BTS1 (324 mg) was obtained in 83% yield. Gel permeation chromatography (GPC): M_w 74600; M_w/M_n 2.4 (Table 1, no. 1). ^{1}H NMR (300 MHz, $CDCl_3$), δ (TMS, ppm): 7.85 (d, 2H, Ar-*H*), 7.71 (m, 4H, Ar-*H*), 2.14 (m, br, 4H, C*H*$_2$), 1.28–1.17 (m, br, 24H, C*H*$_2$), 0.84 (t, 6H, C*H*$_3$). Anal. Calcd: C, 85.40; H, 9.57; N, 2.03. Found: C, 85.04; H, 9.41; N, 2.02. UV-vis ($CHCl_3$), $\lambda_{max}/\varepsilon_{max}$ (mol^{-1} L cm^{-1}): 385 nm/2.1×10^4.

PLED Fabrication and Characterization

The PLEDs were fabricated with a configuration of ITO/PEDOT:PSS/emissive layer/Ba/Al. Polymers were dissolved in toluene and filtered through a 0.45 μm filter. Patterned indium–tin oxide (ITO, ~15 Ω/square)-coated glass substrates were cleaned by routine cleaning procedures, which included sonication in detergent followed by repeated rinsing in distilled water, acetone, and isopropanol, subsequently. After treatment with oxygen plasma, 50 nm of poly(3,4-ethylenedioxythiophene) doped with poly(styrenesulfonic acid) (PEDOT:PSS) (Baytron P 4083, Bayer AG) was spin-coated onto the ITO substrate followed by drying in a vacuum oven at 80°C for 8 h. A thin film of electroluminescent polymer was coated on the PEDOT:PSS layer by spin-casting inside a nitrogen-filled drybox (Vacuum Atmosphere). The film thickness of the emissive layer was around 80 nm, as measured with an Alfa Step 500 surface profiler (Tencor). A thin layer of Ba (4–5 nm) and subsequently a 200 nm layer of Al were evaporated subsequently on the top of the emissive layer under a vacuum of 1×10^{-4} Pa. Device performances were measured inside a drybox (Vacuum Atmosphere). Current-voltage (*I–V*) characteristics were recorded with a Keithley 236 source meter. The luminance of device was measured with calibrated photodiode. The external quantum efficiency was verified by measurement in the integrating sphere (IS-080, Labsphere), and luminance was calibrated by using

a PR-705 SpectraScan spectrophotometer (Photo Research) after encapsulation of the devices with UV-curing epoxy and thin cover glass.

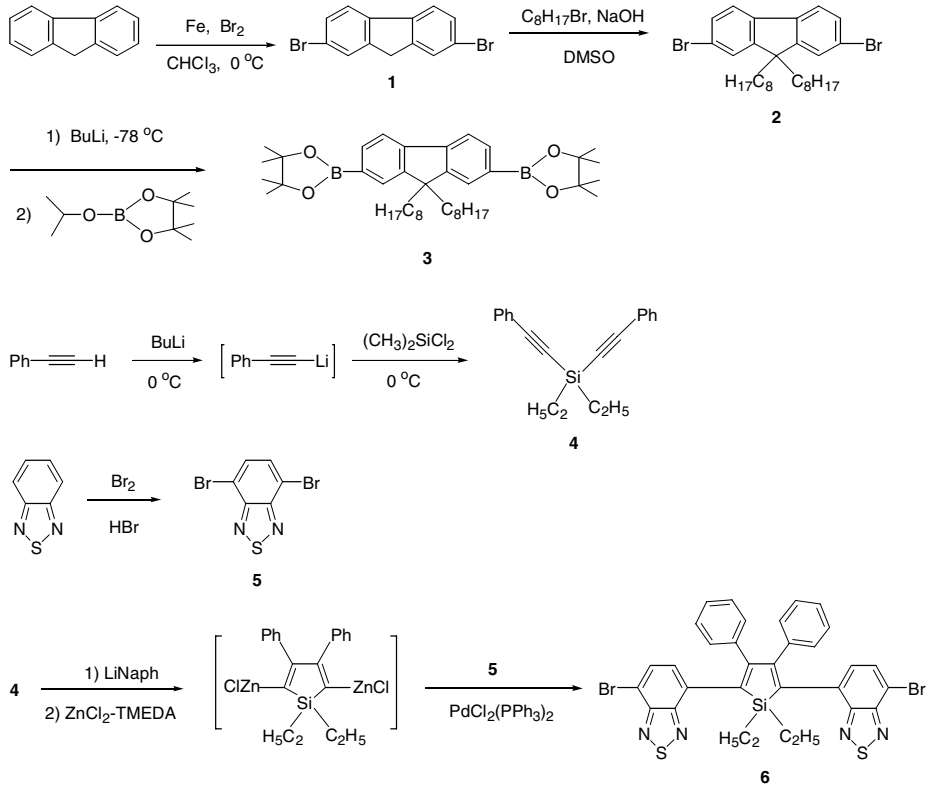

Scheme 1. Synthesis of the monomers.

Results and Discussion

Monomer Synthesis

The synthetic procedures for monomers used in this work are shown in Scheme 1. The two fluorene monomers **2** and **3** were synthesized according to the literature [15]. The 4,7-dibromo-2,1,3-benzothiadiazole **5** was prepared according to the report by Huang et al [28]. The new 2,5-bis(2,1,3-benzothiadiazolyl)silole monomer **6** was prepared by a facile one-pot synthesis route including a reverse addition process. According to Yamaguchi method [29], 2,5-dilithiosilole was prepared by the reaction of bis(phenylethynyl)-diethylsilane **4** with 4 equiv amount of lithium naphthalenide (LiNaph). Further addition of 4 equiv amounts of $ZnCl_2$(tmen) (tmen = *N*,*N*,*N*′,*N*′-tetramethylethylenediamine) readily converted 2,5-dilithiosilole to 2,5-dizincated silole and quenched the excessive LiNaph remained in the system. Subsequently, a reverse addition process was utilized, in which the mixture of the 2,5-dizincated silole was dropwise added to the THF solution of excessive **5** (3 equiv) in the presence of $PdCl_2(PPh_3)_2$ at 55°C within 30 min. The silole monomer **6** was obtained in a yield

of 30% based on diyne **4**. The chemical structure of **6** was confirmed by ^{1}H NMR, ^{13}C NMR, and elemental analysis (see the experimental section for details).

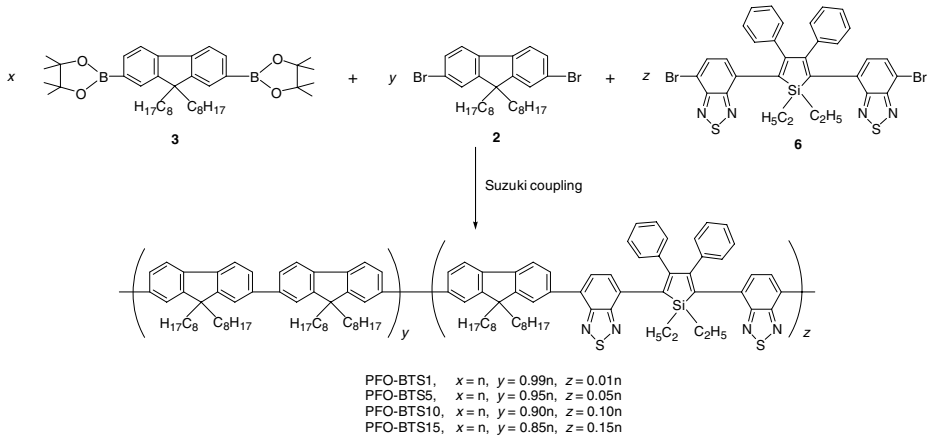

Scheme 2. Polymerization for the copolymers.

Polymerization

Random copolymers in this work was prepared by palladium(0)-catalyzed Suziki coupling reaction with equivalent molar ratio of the diboronic ester **3** to the dibromo monomers (Scheme 2). The molar ratios of the two fluorenes (**2** and **3**) to **6** are 0.99:0.01, 0.95:0.05, 0.90:0.10, and 0.85:0.15 in the feed compositions, and the corresponding copolymers are named PFO-BTS1−15 (Table 1). All the copolymers are soluble in common solvents such as chloroform, toluene, and tetrahydrofuran, etc. The molecular weights of the copolymers are listed in Table 1. The M_w values of the copolymers are between 54.4−83.5 KDa with M_w/M_n from 1.5 to 2.4. The elemental analyses of the copolymers are also listed in Table 1. The C, H, and N contents of the copolymers are very close to those of the feed compositions.

Table 1. Molecular weights and elemental analyses of the copolymer

			elemental analysis[b]		
copolymer	M_w[a]	M_w/M_n[a]	C	H	N
PFO-BTS1	74 600	2.4	87.94 (89.29)	10.42 (10.70)	–
PFO-BTS5	54 400	1.6	87.18 (88.10)	10.07 (10.38)	0.86 (0.71)
PFO-BTS10	83 500	1.6	85.46 (86.70)	9.90 (9.96)	1.39 (1.38)
PFO-BTS15	67 200	1.5	85.04 (85.40)	9.41 (9.57)	2.02 (2.03)

[a] Estimated by GPC in THF on the basis of a polystyrene calibration. [b] Data given in the parentheses are contents in the feed compositions.

UV-vis Absorption and Electrochemical Properties

Figure 1A shows the normalized UV-vis absorption spectra of the chloroform solutions of PFO-BTS1−15. The PFO-BTS1 shows absorption maximum at 385 nm, which can be ascribed to the π–π^* transitions of the fluorene segments. The

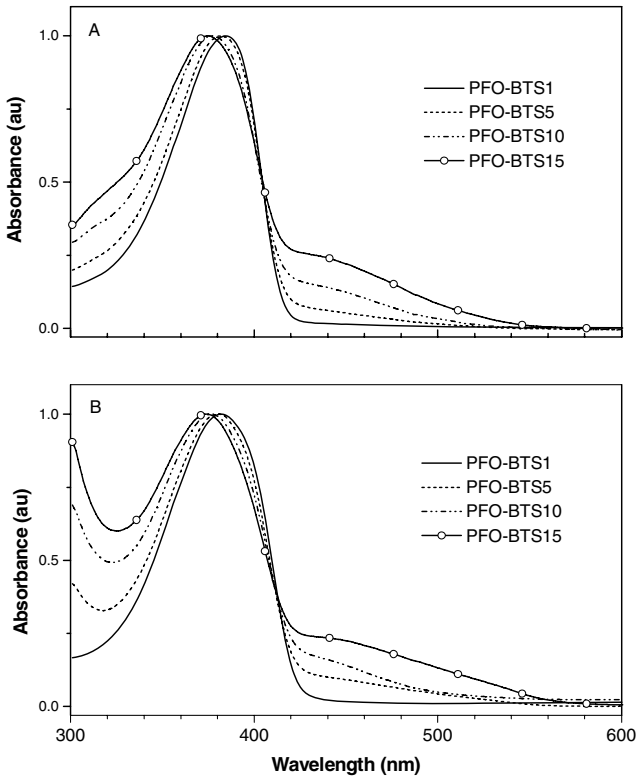

Figure 1. UV-vis absorption spectra of the copolymers: (A) Chloroform solution (1×10^{-4} M), (B) thin solid film.

absorption edge of the copolymer is at around 440 nm. Thus the absorption spectrum of the copolymer is practically identical to that of PF homopolymer due to the very low content (1%) of the BTS in the copolymer [4]. But copolymers PFO-BTS5−15 can show obvious absorptions at longer wavelengths, which are from the contribution of the BTS. The absorption maxima of the copolymers gradually blue-shift to 375 nm while the absorption edges gradually red-shift to 557 nm. The red-shifts of the absorption edges of the copolymers along with the increase of BTS content demonstrate the narrow band gap property of the BTS. The absorption spectra of the films of PFO-BTS1−15 are close to those of their chloroform solutions (Figure 1B), and the optical band gaps of the copolymers are estimated from the onset wavelengths of the absorption spectra of the films and are listed in Table 2. The optical band gaps of the copolymers gradually decrease from 2.79 eV of PFO-BTS1 to 2.13 eV of PFO-BTS15.

The electrochemical behaviors of the films of the copolymers were investigated by cyclic voltammetry (CV). The measurement was performed in a 0.1 M *n*-Bu_4NPF_6 solution in acetonitrile at room temperature. The CV curves were referenced to a saturated calomel electrode (SCE). According to an empirical relation [30], the ionization potential (HOMO) and electron affinity (LUMO) of a conjugated polymer are approximately equal to the onset oxidation potential (vs SCE) and the onset reduction potential (vs SCE) plus 4.4 eV (the SCE energy level below the vacuum

level), respectively. The cyclic voltammograms of the copolymers are shown in Figure 2. The p-doping processes of the copolymers in the CV scans are reversible for the copolymers PFO-BTS5−15 and irreversible for PFO-BTS1. The onsets of oxidation potentials (E_{ox}) of the copolymers are of ~1.29 V (Table 2). The calculated HOMO levels of the copolymers are between −5.67 and −5.71 eV, generally in agreement with those of many fluorene based copolymers. Some reports have found that n-doping process is not reliable to evaluate the LUMO levels of conjugated copolymers and the LUMO level is calculated with the HOMO level and the optical band gap [14,25]. Here the method is also utilized to obtain the LUMO levels of PFO-BTS1−15 and the results are listed in Table 2. The LUMO level values of the copolymers gradually decrease from −2.92 eV of PFO-BTS1 to −3.54 eV of PFO-BTS15.

Table 2. Optical band gaps and electrochemical properties of films of the copolymers

Copolymer	Optical band gap[a] (eV)	E_{ox} (V)	HOMO[b] (eV)	LUMO[c] (eV)
PFO-BTS1	2.79	1.31	−5.71	−2.92
PFO-BTS5	2.28	1.30	−5.70	−3.42
PFO-BTS10	2.25	1.27	−5.67	−3.42
PFO-BTS15	2.13	1.27	−5.67	−3.54

[a] Estimated from the onset wavelength of optical absorption of a film.
[b] Calculated according to HOMO = $-e(E_{ox} + 4.4)$.
[c] Calculated from HOMO level and the optical band gap.

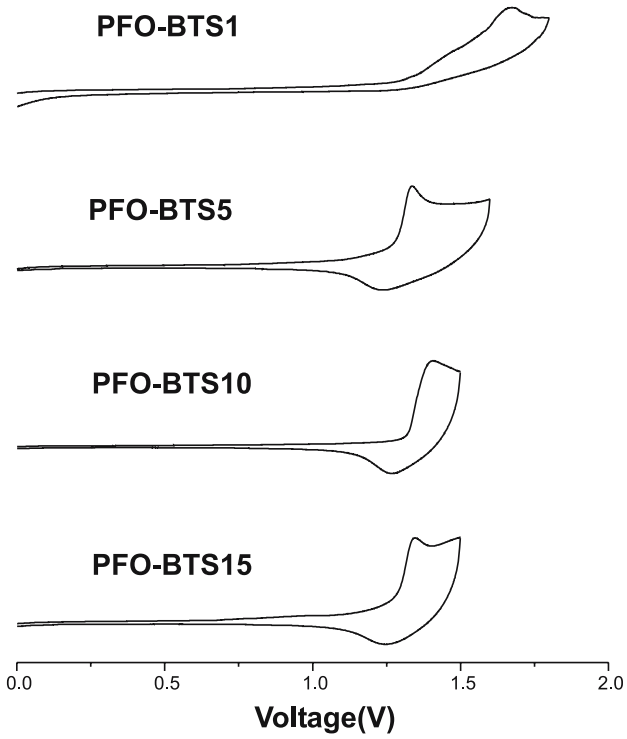

Figure 2. Cyclic voltammetry of films of the copolymers.

Photoluminescence Properties

Photoluminescence spectra of PFO-BTS1–15 in THF solution at a concentration of 4×10^{-5} M are shown in Figure 3A. The PL peak positions (λ_{max}) are listed in Table 3. The PL spectrum of PFO-BTS1 exhibits two well-resolved peaks of the PL emission of a PF homopolymer at 416 and 439 nm, and there is no obvious signature of BTS emission. With the increasing of the content of BTS in the copolymers, new peaks at ~555 nm appear in the PL spectra of PFO-BTS5–15, which can be attributed to BTS emission. The intensities of the new peaks increase when larger amounts of BTS are incorporated in the copolymers.

Figure 3B shows the PL spectra of films (80 nm) of PFO-BTS1–15, and the λ_{max} values are also listed in Table 3. Even for the PFO-BTS1, the blue emission of the fluorene segments is largely weakened and the PL spectrum displays BTS-dominant emission with a main peak at 533 nm. The PL spectrum of PFO-BTS5 shows exclusive BTS emission with λ_{max} at 562 nm. For the copolymers with higher BTS contents, the λ_{max} values gradually red-shift to 566 nm for PFO-BTS10 and 571 nm for PFO-BTS15. Compared with PL spectra of the solutions, the BTS-dominant

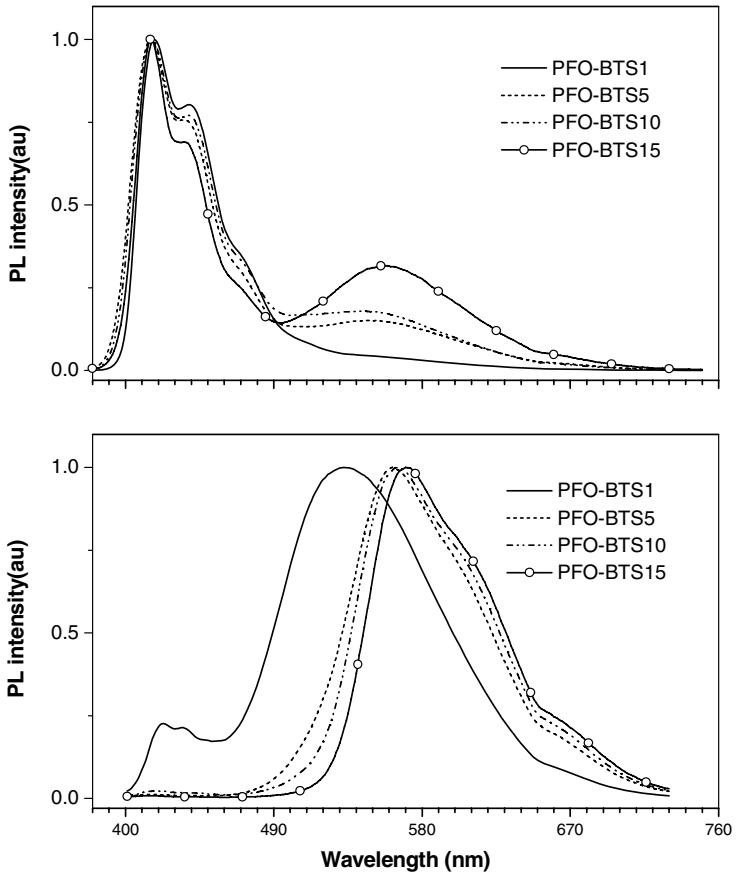

Figure 3. Photoluminescence spectra of the copolymers: (A) THF solution (4×10^{-5} M), (B) thin solid film. Excitation wavelength: 390 nm.

emissions of PFO-BTS1−15 in the solid state should be attributed to the great effect of interchain energy transfer [15] from the fluorene segments to the BTS units. Absolute PL quantum yields (Φ_{PL}) of the films of the copolymers are listed in Table 3. The Φ_{PL} values of PFO-BTS1−15 are between 22 and 34%, higher than those of PFO-TST in a previous report, in which a thiophene is attached on the 2- or 5-positions of the silole [24].

Table 3. PL Properties of the Copolymers[a]

copolymer	solution	film	
	λ_{max} (nm)	λ_{max} (nm)	QE (%)[b]
PFO-TST1	416, 439	423, 533	34
PFO-TST5	416, 439, 553	562	22
PFO-TST10	418, 439, 552	566	29
PFO-TST20	418, 439, 558	571	25

[a] Excitation wavelength: 390 nm. [b] Absolute PL quantum yield measured in the integrating sphere.

Electroluminescence Properties

PLEDs with PFO-BTS1−15 as the emissive layer were fabricated with a configuration of ITO/PEDOT/emissive layer/Ba/Al. The EL spectra are shown in Figure 4. With PFO-BTS1 as the emissive layer, the EL device displays BTS-dominant emission of an orange color with λ_{max} at 574 nm and CIE coordinates of (0.47, 0.50) (Table 4). The blue emission from the fluorene segments in the EL spectrum is weaker compared with that in the PL spectrum of its film. For PFO-BTS5−15 with higher BTS contents, only BTS emissions are found from their EL spectra, and the λ_{max} values gradually

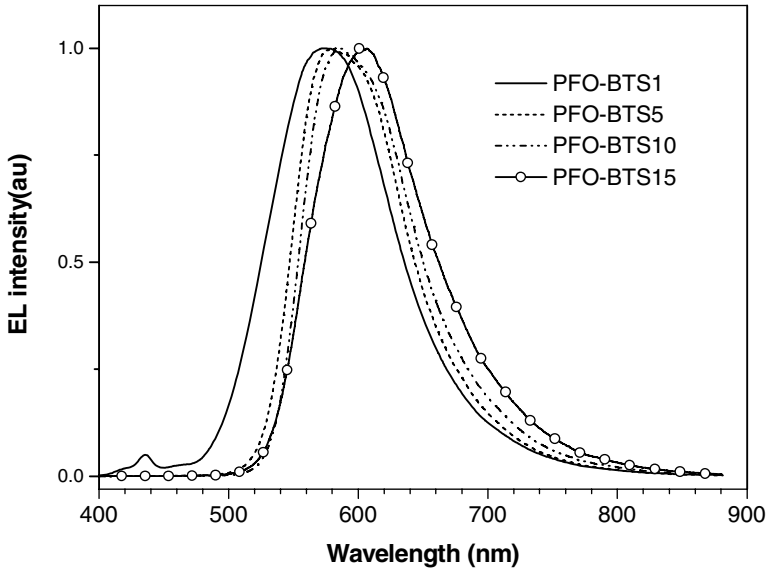

Figure 4. Electroluminescence spectra of the copolymers. Device configuration: ITO/PEDOT/emissive layer/Ba/Al.

Table 4. Electroluminescence properties of the copolymers[a]

No.	Emissive layer	λ_{max} (nm)	CIE (x, y)	bias (V)	current (mA)	brightness (cd/m^2)	η_{EL}[b] (%)
1	PFO-BTS1	574	0.47, 0.50	8.8	8.3	128	0.24
2	PFO-BTS5	583	0.53, 0.46	5.8	5.0	133	0.36
3	PFO-BTS10	587	0.55, 0.44	7.3	5.4	147	0.41
4	PFO-BTS15	601	0.57, 0.43	4.8	5.9	225	0.51
5	PFO-BTS15 : PFO = 1:1	585	0.54, 0.45	6.1	5.9	166	0.42
6	PFO-BTS15 : PFO = 1:2	577	0.49, 0.48	5.9	4.0	329	0.91
7	PFO-BTS15 : PFO = 1:4	571	0.46, 0.49	7.0	6.6	565	0.94
8	PFO-BTS15 : PFO = 1:8	559	0.42, 0.50	6.4	7.2	584	0.88

[a] Device configuration: ITO/PEDOT/emissive layer/Ba/Al.
[b] The external quantum efficiency.

red-shift to 583 nm for PFO-BTS5, 587 nm for PFO-BTS10, and 601 nm for PFO-BTS15, showing better red light CIE coordinates. The results demonstrate that BTS units could be efficient exciton traps. Therefore the largely direct trapping of excitons by the BTS units in the EL process is quite different from the excitation energy transfer in the PL process. Consequently, the EL spectra of the copolymers are red shifted compared with those of the corresponding PL spectra. Similar results had been found for other silole-containing polymers [23,24].

The brightness-current density characteristics of the PLEDs are shown in Figure 5 and the device performances at ~5 mA or ~33 mA/cm^2 of the four copolymers are summarized in Table 4. The η_{EL} values for PFO-BTS1−15 are between 0.24 and 0.51%. It should be noted that red light EL emissions from silole-containing polymer

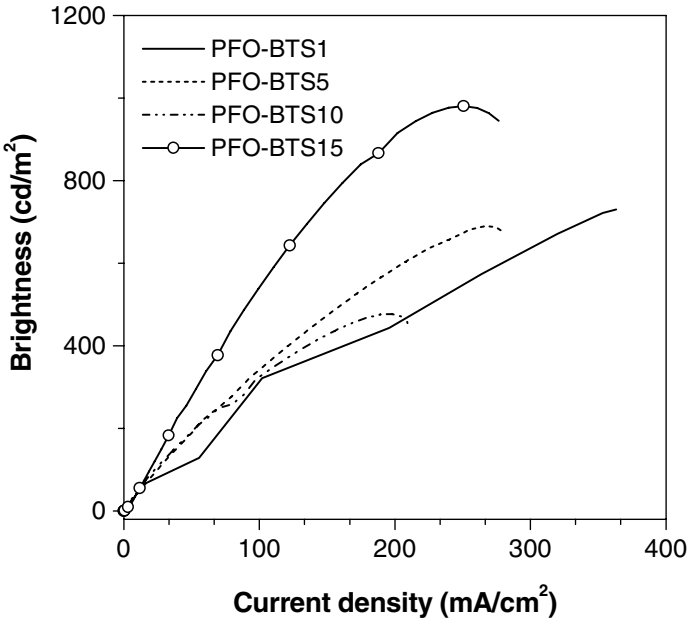

Figure 5. Brightness-current density characteristics of the PLEDs with PFO-BTS1−15 as the emissive layer. Device configuration: ITO/PEDOT/emissive layer/Ba/Al.

are rather rare [24,31]. The efficiencies of PFO-BTS1−15 are generally higher than those of PFO-TST with a same device configuration in a previous report [24], possibly due to the contribution of electron transporting ability of the BT heterocycle. Compared with the other three PLEDs, the device with PFO-BTS15 as the emissive layer displays the higher brightness and efficiency in a wide current density range (Figure 5). The maximum brightness of the device reaches 980 cd/m^2 at a current density of 251 mA/cm^2.

In a previous paper, we reported that the EL efficiency of a red-emitting PF copolymer could be improved by blending with PFO, a PF homopolymer [32]. Here PFO-BTS15 was utilized to fabricate blend-type PLEDs with the PFO. Solution blends with weight ratios of PFO-BTS15:PFO = 1:1, 1:2, 1:4, and 1:8 were tested (Table 4, nos. 5−8). The brightness-current density characteristics of the PLEDs are shown in Figure 6 and the device performances at ~5 mA are also summarized in Table 4 for comparison. With PFO-BTS15:PFO = 1:1 blend as the emissive layer, there is no improvement of the EL efficiency. But for the PFO-BTS15:PFO = 1:2 blend, the brightness of the device is much higher than that of the neat film. Consequently the η_{EL} of the device is boosted to 0.91% (Table 4, no. 6). With the PFO-BTS15:PFO = 1:4 blend as the emissive layer, the η_{EL} of the device is 0.94% at a current of 6.6 mA (Table 4, no. 7). A maximum η_{EL} of 1.37% of the device is realized at a lower current of 2.75 mA, showing a brightness of 341 cd/m^2. Further increasing the ratio of PFO-BTS15:PFO to 1:8, the device shows a slight decrease of η_{EL}. For the blends with ratios of PFO-BTS15:PFO from 1:2 to 1:8, the values for the maximum brightness of the devices are all higher than 2000 cd/m^2 (Figure 6), with obvious improvements over the those of the neat films. The λ_{max} values of the blend-type PLEDs show blue-shifting with the increasing of PFO content

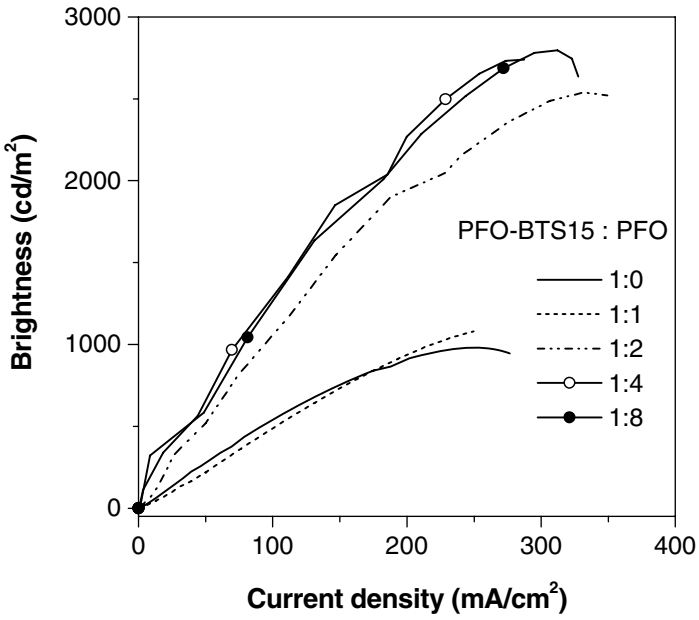

Figure 6. Brightness-current density characteristics of the PLEDs with PFO-BTS15/PFO blends as the emissive layer. The curve for the neat film of PFO-BTS15 is remained for comparison. Device configuration: ITO/PEDOT/emissive layer/Ba/Al.

in the blends. The improved EL efficiencies and the increased brightness of the devices with some PFO-BTS15/PFO blends as the emissive layer should be due to balanced charge injection and transport. The possibility for the BTS located on the copolymer chains to capture excitons generated on the PFO chains would also be increased in a blend with a higher PFO content.

Conclusions

In this work, BTS, a new silole monomer with bulky electron-deficient benzothiadiazole heterocycles at 2,5-positions, was prepared by a facile one-pot synthesis route, from which soluble conjugated random copolymers PFO-BTS were successfully synthesized by Suziki coupling reactions. The interchain excitation energy transfer could be largely enhanced in the solid state, giving BTS-dominant PL emissions. EL devices of the copolymers with a configuration of ITO/PEDOT/copolymer/Ba/Al displayed orange-red emissions with λ_{max} up to 601 nm and the highest EL efficiency was achieved by PFO-BTS15. Using the PFO-BTS15:PFO = 1:4 blend as the emissive layer, a maximum external quantum efficiency of 1.37% was realized.

Acknowledgement. This work was partially supported by National Natural Science Foundation of China (Grant nos. 50303006 and 50433030), Special Funds for Major State Basic Research Projects (Grant no. 2002CB613404), and Education Ministry of China (Program for NCET).

References

1. Grice A W, Bradley DDC, Bernius MT, Inbasekaran M, Wu WW, Woo EP (1998) Appl Phys Lett 73:629
2. Scherf U, List EJW (2002) Adv Mater 14:477
3. Wu FI, Shih PI, Shu CF, Tung YL, Chi Y (2005) Macromolecules 38:9028
4. Ranger M, Rondeau D, Leclerc M (1997) Macromolecules 30:7686
5. Liu, B.; Yu, W. L.; Lai, Y. H.; Huang, W. *Macromolecules* 2000, *33*, 8945
6. Wu FI, Shih PI, Tseng YH, Chen GY, Chien CH, Shu CF, Tung YL, Chi Y, Jen AKY (2005) J Phys Chem B 109:14000
7. Kulkarni AP, Kong X, Jenekhe SA (2004) J Phys Chem B 108:8689
8. Liu J, Zhou Q, Cheng Y, Geng Y, Wang L, Ma D, Jing X, Wang F (2005) Adv Mater 17:2974
9. Liu J, Zhou Q, Cheng Y, Geng Y, Wang L, Ma D, Jing X, Wang F (2006) Adv Funct Mater16:957
10. Mei C, Tu G, Zhou Q, Cheng Y, Xie Z, Ma D, Geng Y, Wang L (2006) Polymer 47:4976
11. Chang SW, Hong JM, Hong JW, Cho HN (2001) Polym Bull 47:231
12. Jung SH, Suh DH, Cho HN (2003) Polym Bull 50:251
13. Zhang H, Chen H, Li Y, Jiang Q, Xie M (2006) Polym Bull 57:121
14. Hou Q, Xu Y, Yang W, Yuan M, Peng J, Cao Y (2002) J Mater Chem 12:2887
15. Yang R, Tian R, Yang W, Hou Q, Cao Y (2003) Macromolecules 36:7453
16. Yang J, Jiang C, Zhang Y, Yang R, Yang W, Hou Q, Cao Y (2004) Macromolecules 37:1211
17. Lee J, Jung BJ, Lee SK, Lee JI, Cho HJ, Shim HK (2005) J Polym Sci Part A: Polym Chem 43:1945
18. Cho NS, Hwang DH, Jung BJ, Lim E, Lee J, Shim HK (2004) Macromolecules 37:5265
19. Chen J, Law CCW, Lam JWY, Dong Y, Lo SMF, Williams ID, Zhu D, Tang BZ (2003) Chem Mater 15:1535

20. Chen J, Xie Z, Lam JWY, Law CCW, Tang BZ (2003) Macromolecules 36:1108
21. Chen J, Xu B, Yang K, Cao Y, Sung HHY, Williams ID, Tang BZ (2005) J Phys Chem B 109:17086
22. Chen HY, Lam JWY, Luo JD, Ho YL, Tang BZ, Zhu DB, Wong M, Kwok HS (2002) Appl Phys Lett 81:574
23. Wang F, Luo J, Chen J, Huang F, Cao Y (2005) Polymer 46:8422
24. Wang F, Luo J, Yang K, Chen J, Huang F, Cao Y (2005) Macromolecules 38:2253
25. Wang Y, Hou L, Yang K, Chen J, Wang F, Cao Y (2005) Macromol Chem Phys 206:2190
26. Uchida M, Izumizawa T, Nakano T, Yamaguchi S, Tamao K, Furukawa K (2001) Chem Mater 13:2680
27. Campbell AJ, Bradley DDC, Antoniadis H (2001) Appl Phys Lett 79:2133
28. Huang J, Niu Y, Yang W, Mo Y, Yuan M, Cao Y (2002) Macromolecules 35:6080
29. Yamaguchi S, Endo T, Uchida M, Izumizawa T, Furukawa K, Tamao K (2000) Chem Eur J 6:1683
30. Li Y, Ding J, Day M, Tao Y, Lu J, Diorio M (2004) Chem Mater 16:2165
31. Ohshita J, Hamamoto D, Kimura K, Kunai A (2005) J Organomet Chem 690:3027
32. Iuo J, Hou Q, Chen J, Cao Y (2006) Synth Met 156:470